

LAIR-1 overexpression inhibits osteosarcoma epithelial-mesenchymal transition via GLUT1-related energy metabolism

Jinxue Zhang

Fourth Military Medical University

Yuan Zhang

Fourth Military Medical University <https://orcid.org/0000-0002-2754-1291>

Yongming Liu

Fourth Military Medical University

Xin Yi

Fourth Military Medical University

Shiyang Cheng

Fourth Military Medical University

Dongxu Jiang

Fourth Military Medical University

Yong Ding

Fourth Military Medical University

Ran Zhuang (✉ fmmuzhr@fmmu.edu.cn)

Research

Keywords: Osteosarcoma, leukocyte-associated immunoglobulin-like receptor-1, epithelial-mesenchymal transition, glucose transporter 1

Posted Date: February 12th, 2020

DOI: <https://doi.org/10.21203/rs.2.23323/v1>

License: © ⓘ This work is licensed under a Creative Commons Attribution 4.0 International License.

[Read Full License](#)

Version of Record: A version of this preprint was published on June 20th, 2020. See the published version at <https://doi.org/10.1186/s12957-020-01896-7>.

Abstract

Background: Leukocyte-associated immunoglobulin-like receptor-1 (LAIR-1) is a collagen receptor belonging to the immunoglobulin superfamily. Although prior studies have evaluated the biological role of LAIR in solid tumors, the precise mechanisms underlying LAIR-1 functions as a regulator of tumor biological functions remains unclear. **Methods:** LAIR-1 expression was evaluated using an osteosarcoma (OS) tissue microarray by immunohistochemical analysis. Wound healing and Transwell assays were performed to evaluate tumor cell migration. Quantitative PCR and western blotting were conducted to detect the expression of epithelial-mesenchymal transition (EMT)-related molecules. RNA-sequencing (RNA-seq) was conducted to evaluate the mRNA expression profiles after overexpressing LAIR-1 in OS cells. Glucose uptake and glucose transporter (Glut) 1 expression in OS cells in vitro were evaluated by flow cytometry and western blotting. **Results:** LAIR-1 expression significantly differed between the T1 and T2 stages of OS tumors, and LAIR-1 overexpression inhibited OS cell migration. LAIR-1 expression was inversely correlated with the expression of EMT-associated transcription factors via the Forkhead box O1/Twist1 signal transduction pathway. Furthermore, RNA-seq and quantitative PCR demonstrated that EMT energy metabolism-related molecules were significantly reduced after LAIR-1 overexpression. **Conclusions:** Notably, overexpression of LAIR-1 in OS cells decreased Glut1 expression. These findings provide insight into the molecular mechanism underlying OS progression.

1. Background

Osteosarcoma (OS) is the most common malignant solid bone tumor in children and young adults, accounting for 6% of all pediatric cancers and typically originating in the metaphyses of long bones [1, 2]. Multidisciplinary approaches have been developed for treating patients with OS [3, 4]; however, their overall prognosis remains unsatisfactory, with a 5-year survival rate as low as 20% [5–7]. Therefore, new and effective targets for OS diagnosis, therapy, and prognosis are needed.

Leukocyte-associated immunoglobulin-like receptor-1 (LAIR-1; also known as CD305) is a collagen receptor and member of the immunoglobulin superfamily [8]. Studies to evaluate the functions of LAIR-1 have mainly focused on immune cells, such as T cells, B cells, natural killer (NK) cells, monocytes, megakaryocytes, and CD34⁺ hematopoietic progenitor cells [9]. LAIR-1 is important in several different types of cancer including leukemia and solid tumors [10–14].

In this study, we measured LAIR-1 expression in OS tissues to evaluate the roles of LAIR-1 in OS progression. We overexpressed LAIR-1 in OS cell lines by lentiviral transfection, and then measured cell proliferation, epithelial-mesenchymal transition (EMT)-associated transcription factor expression, and cell migration. Furthermore, EMT-related energy metabolism was examined after LAIR-1 overexpression. Our study provides insight into the role of LAIR-1 in OS.

2. Materials And Methods

2.1. Immunohistochemistry (IHC)

We used a formalin-fixed paraffin-embedded tissue microarray comprising 62 samples from patients with OS and nine samples from adjacent normal rib bone tissues (Alenabio Biological Technology Company; Xi'an, Shaanxi, China). Clinicopathological data were collected from the medical records of surgically treated patients with OS, including age, sex, pathological diagnosis, TNM grading, and stage. No patients had been administered preoperative treatment or had the co-occurrence of other diagnosed tumors. The sample size of patients with the T3 stage was small ($n = 3$), and thus this group was excluded from analysis. Samples for IHC were prepared using a standard method.

2.2. Semi-quantitative analysis of immunohistochemical data and bioinformatics analysis

All tissue samples were evaluated by two independent pathologists blinded to the clinical data. A semi-quantitative score was generated based on the IHC staining intensity as follows: +, weak staining; ++, moderate staining; +++, intense staining. The R2 platform (<http://r2.amc.nl>) was used to analyze the public OS dataset, which includes 127 OS samples.

2.3. Cell culture

Human OS cell lines were purchased from ATCC (Manassas, VA, USA), and the human normal osteoblast cell line hFOB1.19 was obtained from Jennio Biotech (Guangzhou, Guangdong, China). All cells were cultured at 37 °C in a humidified atmosphere containing 5% CO₂. Foxo1 short interfering RNA (siRNA) and negative control siRNA were purchased from Santa Cruz Biotechnology (Dallas, TX, USA). Cells were transfected with 50 nM siRNA or negative control (NC) siRNA using Lipofectamine 3000 according to the manufacturer's protocol (Invitrogen, Carlsbad, CA, USA).

2.4. Lentivirus infection

Commercially available lentiviral LV-LAIR-1 constructs (Tianyucheng Biotechnology, Xi'an, Shaanxi, China) were modified to overexpress LAIR-1. Human OS cells were infected with LV-negative control (LV-NC) or LV-LAIR-1. The infection efficiency of lentiviral vectors expressing green fluorescent protein (GFP) was evaluated by fluorescence microscopy.

2.5. Quantitative PCR (qPCR) assay

Total RNA was extracted from cells using TRIzol Reagent (Invitrogen). SuperScript III Reverse Transcriptase (Invitrogen) was used for reverse transcription, and PCR was performed using SYBR Green Realtime PCR Master Mix (TAKARA, Shiga, Japan). The qPCR primers for human genes were purchased from Tsingke Biotech (Beijing, China). Relative gene expression was quantified using the comparative Ct method ($2^{-\Delta\Delta CT}$) with GAPDH used as an internal control.

2.6. Western blotting

Total protein was prepared using a routine procedure and blotted with following primary antibodies: LAIR-1 (sc-398141; Santa Cruz Biotechnology), phospho-FoxO1 (Ser256) (84192; Cell Signaling Technology, Danvers, MA, USA), FoxO1 (2880; Cell Signaling Technology), phospho-Akt (Ser473) (AF8355; Affinity Biosciences, Cincinnati, OH, USA), Akt (9272; Cell Signaling Technology), proliferating cell nuclear antigen (PCNA; BM0104; Boster Biotech Co., Ltd., Wuhan, China), Twist1 (ab50581; Abcam, Cambridge, UK), Glut1 (NB110-39113, Novus Biologicals, Littleton, CO, USA), and β -actin (30101ES50; Yeasen Biotech Co., Ltd., Shanghai, China).

2.7. Wound healing and Transwell migration assays

Cells were seeded into six-well plates, and a scratch was produced in the monolayer after 48 h. Images of the wound area were captured immediately after the scratch and after 6 and 12 h (T0, T6, and T12, respectively) to monitor cell migration into the wounded area. The percentage of the scratch area (% scratch) that had closed was calculated as follows: (width at T0 - width at T6 or T12)/width at T0 \times 100.

A Transwell migration assay was performed using a Transwell chamber with 8- μ m pores (Millipore, Billerica, MA, USA). Untreated OS cells (blank) and their corresponding transfectants overexpressing LV-NC and LV-LAIR-1 were seeded (2×10^4 into each well) into the upper chambers in 500 μ L serum-free medium. The lower chambers were filled with complete medium, and all chambers were incubated at 37 °C for 24 h. The cells on the upper surface of the membrane were removed, and those in the lower chamber were fixed and stained with 0.1% crystal violet. Images were obtained using an inverted microscope (CX41, Olympus, Tokyo, Japan).

2.8. Immunofluorescent staining

Cells were cultured on glass chamber slides. The cells were fixed and permeabilized, and then incubated with primary antibodies for 1 h at room temperature. After washing, the cells were incubated with Cy3-labeled goat anti-rabbit secondary antibody and stained with DAPI (Roche Diagnostics, Basel, Switzerland). Images were obtained using an Olympus microscope. Immunofluorescence intensities were quantified using ImageJ software (NIH, Bethesda, MD, USA).

2.9. RNA-sequencing (RNA-seq)

Total RNA was extracted from HOS cells transfected with LV-NC (n = 3) and LV-LAIR-1 (n = 3) using an RNeasy Micro kit (Qiagen, Hilden, Germany) according to the manufacturer's instructions. RNA was quantified using a Nano Drop ND-2000 (Nanodrop Technologies, Inc., Wilmington, DE, USA). Generation of the transcriptome library and RNA-seq were performed on the BGISEQ platform (BGI Technologies, Shenzhen, China). The Dr. TOM2 system was used to analyze the transcriptome data.

2.10. Statistical analysis

Data were statistically analyzed using GraphPad Prism version 5.0 software (GraphPad, Inc., La Jolla, CA, USA); all data are presented as the mean \pm standard deviation. Data were analyzed using an independent sample t-test for comparisons between two groups. Clinical data were statistically analyzed using SPSS

software (version 10.0; SPSS, Inc., Chicago, IL, USA). The Pearson χ^2 test was used to evaluate the statistical significance of the association between LAIR-1 expression and clinical features (n = 59). Statistical significance was defined as P < 0.05.

3. Results

3.1 Increased LAIR-1 expression is associated with advanced T stage in patients with OS

IHC staining was performed to detect LAIR-1 expression in 62 human OS samples and 9 adjacent normal bone tissues. Unlike the membrane expression pattern in lymphocytes, which have a large nucleus and small cytoplasmic volume, we observed higher LAIR-1 expression in the cytoplasm of OS cells than in the cell membrane (Fig. 1A). Comparisons between LAIR-1 expression and the clinicopathological characteristics of patients with OS are shown in Table 1. LAIR-1 expression was significantly higher in patients in the T2 stage than in those in the T1 stage of OS tumors (P = 0.006).

Table 1
Relationship between LAIR-1 expression and clinicopathological features in OS patients (n = 59).

Variable		No. of patients	LAIR-1 expression			P values
			+	++	+++	
Gender	Male	37 (62.7)	7	14	16	0.871
	Female	22 (37.3)	3	9	10	
Age	≥ 20	38 (64.4)	3	16	19	0.037
	< 20	21 (35.6)	7	5	9	
T stage	T1	17 (28.8)	7	5	5	0.006
	T2	42 (71.2)	3	16	23	
P values based on χ^2 test; bold, statistically significant (P < 0.05).						

Moreover, analysis of 127 OS samples using the R2 platform indicated that cases with higher levels of LAIR-1 expression had better survival rates than cases with lower LAIR-1 expression levels (P = 0.015, Fig. 1B). According to these observations, we investigated the association between LAIR-1 overexpression and human OS growth and examined whether LAIR-1 overexpression is a compensatory effect to help overcome tumor progression.

3.2. LAIR-1 overexpression inhibited OS cell migration

We compared LAIR-1 expression levels in human OS cell lines and the human osteoblast cell line hFOB1.19 (Supplementary Fig. 1A). To investigate the biological function of LAIR-1 overexpression in OS pathogenesis, we designed a recombinant lentivirus to overexpress LAIR-1 in OS cell lines with low LAIR-1 expression (HOS and SJSA-1). The GFP-positive cell ratio detected in these cells by fluorescence microscopy was over 95% (Supplementary Fig. 1B), demonstrating that the LV-LAIR-1 lentivirus had a high transduction efficiency for HOS cells. LAIR-1 overexpression at the mRNA and protein levels in HOS cells was confirmed by qPCR (Supplementary Fig. 1C) and western blotting (Fig. 1C), respectively.

Additionally, western blotting revealed no differences in the expression of PCNA, a protein marker related to cell proliferation, among all groups (Fig. 1C). An EdU assay and western blotting for PCNA were performed to analyze whether LAIR-1 overexpression affects the growth and proliferation of human OS cells. The EdU assay revealed no difference in the number of positively stained HOS cells between the LAIR-1 overexpression group and LV-NC or blank groups (Supplementary Fig. 1D). These findings demonstrate that LAIR-1 overexpression did not affect OS cell growth or proliferation.

Next, we investigated the effect of LAIR-1 expression on OS metastasis in wound-healing and Transwell assays. The scratch assay showed a significantly lower repair efficiency in LAIR-1-overexpressing cells than in LV-NC-overexpressing and untreated control cells (Fig. 2A). The results of statistical analysis of the scratch closure ratios at 6 and 12 h are shown in Fig. 2B. We also conducted a cell migration assay to analyze the migration ability of OS cells after ectopic LAIR-1 overexpression. The results indicated that the migration ability of OS cells infected with LV-LAIR-1 was dramatically lower than that of LV-NC and untreated blank cells (Fig. 2C and D). These results demonstrate that LAIR-1 overexpression inhibits OS cell migration.

3.3. LAIR-1 overexpression suppressed EMT in OS cells

We further explored the mechanism underlying the suppression of OS cell migration by LAIR-1 overexpression. By qPCR, E-cadherin mRNA expression was found to be upregulated and N-cadherin mRNA expression was downregulated in LAIR-1-overexpressing cells compared to in blank and LV-NC control group cells (Fig. 2E and F); however, no change was observed in vimentin mRNA expression in LAIR-1-overexpressing OS cells (Fig. 2G).

Here, LAIR-1 overexpression significantly decreased the mRNA and protein levels of Twist1 in HOS cells compared to in control cells (Fig. 3A and B). Additionally, immunofluorescence staining revealed that Twist1 expression was significantly downregulated after LAIR-1 overexpression in HOS cells (Fig. 3D).

Evaluation of the Foxo1 levels in OS cells showed that LAIR-1 overexpression decreased Foxo1 phosphorylation; immunofluorescence staining further demonstrated increased nuclear retention of Foxo1 (Fig. 3B and E). Phosphorylation of Akt, the direct upstream regulator of Foxo1, was markedly decreased in LAIR-1-overexpressing OS cells, indicating that decreased Foxo1 phosphorylation and increased Foxo1 retention in the nucleus are regulated by decreased Akt activation.

The role of Foxo1 in reducing Twist1 was further confirmed in OS cells. Twist1 expression was decreased in HOS cells transfected with Foxo1 siRNA compared to in control siRNA-transfected cells (Fig. 3C). These results suggest that LAIR-1 overexpression significantly decreased the EMT in OS cells via Twist1, which functions downstream of phosphorylated Foxo1.

3.4. Characterization of EMT-related genes in LAIR-1-overexpressing OS cells

To further clarify the mechanism involved in the LAIR-1-related EMT process, RNA-seq was performed to detect the mRNA expression profiles in OS cells (reference genome: GCF_000001405.38_GRCh38.p12). We identified 974 mRNAs expressed specifically in LAIR-1-overexpressing OS cells and 1064 mRNAs in NC control by RNA-seq analysis. Compared to the LV-NC control group, 399 mRNAs showed significantly differential expression in LAIR-1-overexpressing OS cells (131 up-regulated and 154 down-regulated, log₂ fold-change \geq 1.0 and false discovery rate < 0.05). The details are presented in Supplementary Table 1. A heatmap was generated to show the respective hierarchical clustering of mRNA with altered levels in OS cells from the LV-NC control and LV-LAIR-1 groups (Fig. 4A).

Furthermore, Kyoto Encyclopedia of Gene and Genomes (KEGG) pathway analysis of the top 20 enriched mRNAs potentially acting on target genes and regulating OS progression were identified (Fig. 4B). Interestingly, several mRNAs reported to play key roles in the EMT were significantly reduced in LAIR-1-overexpressing OS cells (Fig. 4C); these included angiotensin-like (ANGPTL) 4, stanniocalcin (STC) 1, and poly ADP-ribose transferase (PARP) 2.

3.5. LAIR-1 inhibits EMT via Glut1-related energy metabolism

The three RNAs differently expressed between the two groups were validated by qPCR, and the results agreed with the RNA-seq data (Fig. 4D). The EMT is an energy-demanding process fueled by glucose metabolism-derived ATP. Notably, ANGPTL4, STC1, and PARP2 are involved in energy metabolism in the EMT. These data suggest that overexpression of LAIR-1 inhibits the EMT via metabolic-related processes. The EMT is accompanied by up-regulated glucose consumption, as evidenced by up-regulated Glut1 expression [15]. Here, we observed significantly decreased Glut1 in LAIR-1-overexpressing OS cells compared to in controls (Fig. 4E). As shown in Fig. 4F, immunofluorescence staining assay also demonstrated reduced Glut1 expression in LAIR-1 highly expressed OS cells. These results indicate that LAIR-1 is involved in the tumor EMT via a Glut1-related energy metabolism process.

4. Discussion

The inhibitory receptor LAIR-1 is a member of the immunoglobulin superfamily and binds extracellular matrix collagens as high-affinity ligands [16]. Functionally, LAIR-1 tyrosine-based inhibition motifs utilize tyrosine phosphorylation to recruit phosphatases and negatively regulate the immune response and cell differentiation [17]. Additionally, the interaction between LAIR-1 and collagen can facilitate the binding of

tumor cells to inhibitory molecules on immune cells to inhibit antitumor immune responses, suggesting their role in tumor immune evasion [18]. Previous studies demonstrated the biological role of LAIR-1 in solid tumors including ovarian cancer, cervical cancer, and hepatocellular carcinoma.

Although OS is a mesenchymal-derived tumor type, studies have demonstrated an association between the EMT and OS migration [19]. Interestingly, the collagen matrix can induce the EMT transition in OS cells via extracellular signal-regulated kinase (ERK) signaling [20]. As an important collagen ligand, LAIR-1 expression on tumors may regulate the EMT in OS cells. Here, LAIR-1 overexpression was found to decrease N-cadherin expression but did not affect the expression of vimentin. Previous studies reported elevated Twist1 expression in OS tissues, and metastatic OS (phase III) showed higher Twist expression than non-metastatic OS (phase I/II) [21]. Furthermore, Foxo1 inhibits cell migration and invasion and represses the EMT transition in tumors via Snail, Slug, Twist, and zinc finger E-box-binding homeobox 1 signaling [22]. In this study, we found that LAIR-1 overexpression interfered with Foxo1/Twist1 signaling; thus, the LAIR-1/Foxo1/Twist1 feedback loop may be a novel mechanism underlying OS cell migration and the EMT.

Tumor cells exhibit accelerated metabolism, high energy requirements, and increased glucose uptake. ANGPTL4 plays a key role in coordinating the increased cellular energy influx crucial for the EMT. Knockdown of ANGPTL4 suppressed adenylate energy charge elevation, delaying the EMT [23]. Up-regulated of ANGPTL4 predicts poor prognosis in cancers and promotes tumor cell proliferation and migration, including in OS cells [24, 25]. STC1, together with STC-2, was originally identified as a calcium/phosphate-regulating hormone. Recent studies indicated that the STC-1 gene is closely related to glucose and lipid metabolism, as well as to mitochondrial function [26, 27]. Additionally, PARP or PAR alterations have been described in tumors, specifically those influencing the EMT [28–30]. Our RNA-seq and qPCR results strongly suggest that LAIR-1 inhibits the EMT through metabolic pathways.

Glucose metabolism in cancer cells contributes to their proliferation, metastasis, and therapy resistance [31, 32]. Glut1 is abundantly expressed in cancer cells and plays a pivotal role in the glucose metabolism of tumors [33]. Overexpression of LAIR-1 in OS cells inhibits Glut1 expression and may further regulate the glucose metabolism.

5. Conclusions

Together, our findings demonstrate that LAIR-1 is overexpressed in human OS tissues and its expression is significantly higher in the T2 stage than in the T1 stage of OS tumors. LAIR-1 overexpression remarkably reduces OS cell migration and the EMT via Twist1 regulation. Evaluation of the underlying molecular mechanism revealed a regulatory role for LAIR-1 in Glut1-related glucose metabolism. Thus, LAIR1 is a potential diagnostic and prognostic marker and therapeutic target for OS.

Declarations

Abbreviations

ANGPTL4, angiopoietin-like 4; EMT, epithelial-mesenchymal transition; ERK, extracellular signal-regulated kinase; Foxo1, Forkhead box 1; Glut, glucose transporter; IHC, immunohistochemistry; KEGG, Kyoto Encyclopedia of Gene and Genomes; LAIR-1, leukocyte-associated immunoglobulin-like receptor-1; NK, natural killer; OS, osteosarcoma; PARP, poly ADP-ribose transferase; PCNA, proliferating cell nuclear antigen; RNA-seq, RNA-sequencing; STC, stanniocalcin

Ethical approval and consent to participate

This study was exempt from evaluation because human samples were purchased from commercial sources (Research Ethics Committee of the Tangdu Hospital, Fourth Military Medical University). The supplier confirms that the patients provided consent for the collection and use of the samples for this tissue microarray.

Consent for publication

Not applicable.

Availability of data and material

All data generated or analysed during this study are included in this published article.

Competing interests

The authors declare that they have no competing interests.

Funding

This investigation was supported by the Natural Science Foundation of China (No. 81671575 and No. 81871258).

Authors' Contributions

YD and RZ designed the study. JZ, YZ and YL performed the in vitro experiments. XY and SC prepared the figures. DJ collected and analyzed the data. YZ, RZ wrote the manuscript. All authors read and approved the final manuscript.

Acknowledgements

The authors would like to express their sincere thanks to Dr. Shirong Ma for the assistance in pathological diagnosis.

References

1. Han K, Zhou Y, Gan ZH, Qi WX, Zhang JJ, Fen T, Meng W, Jiang L, Shen Z, Min DL: **p21-activated kinase 7 is an oncogene in human osteosarcoma.** *Cell Biol Int* 2014, **38**(12):1394-1402.
2. Dong X, Lv B, Li Y, Cheng Q, Su C, Yin G: **MiR-143 regulates the proliferation and migration of osteosarcoma cells through targeting MAPK7.** *Arch Biochem Biophys* 2017, **630**:47-53.
3. Tetreault MP, Yang Y, Katz JP: **Kruppel-like factors in cancer.** *Nat Rev Cancer* 2013, **13**(10):701-713.
4. Ma H, Su R, Feng H, Guo Y, Su G, Ma H, Su R, Feng H, Guo Y, Su G: **Long noncoding RNA UCA1 promotes osteosarcoma metastasis through CREB1-mediated epithelial-mesenchymal transition and activating PI3K/AKT/mTOR pathway.** *J Bone Oncol* 2019, **16**:100228.
5. Zhang L, Zhang L, Xia X, He S, He H, Zhao W: **Kruppel-like factor 4 promotes human osteosarcoma growth and metastasis via regulating CRYAB expression.** *Oncotarget* 2016, **7**(21):30990-31000.
6. Liu Y, Zhang F, Zhang Z, Wang D, Cui B, Zeng F, Huang L, Zhang Q, Sun Q: **High expression levels of Cyr61 and VEGF are associated with poor prognosis in osteosarcoma.** *Pathol Res Pract* 2017, **213**(8):895-899.
7. Xu G, Guo Y, Xu D, Wang Y, Shen Y, Wang F, Lv Y, Song F, Jiang D, Zhang Y *et al*: **TRIM14 regulates cell proliferation and invasion in osteosarcoma via promotion of the AKT signaling pathway.** *Sci Rep* 2017, **7**:42411.
8. Meyaard L: **The inhibitory collagen receptor LAIR-1 (CD305).** *J Leukoc Biol* 2008, **83**(4):799-803.
9. Zhang Y, Sun H, Li J, Rong Q, Ji X, Li B: **The leukocyte-associated immunoglobulin (Ig)-like receptor-1 modulating cell apoptosis and inflammatory cytokines secretion in THP-1 cells after Helicobacter pylori infection.** *Microb Pathog* 2017, **109**:292-299.
10. Wu X, Zhang L, Zhou J, Liu L, Fu Q, Fu A, Feng X, Xin R, Liu H, Gao Y *et al*: **Clinicopathologic significance of LAIR-1 expression in hepatocellular carcinoma.** *Curr Probl Cancer* 2019, **43**(1):18-26.
11. Wang Y, Zhang X, Miao F, Cao Y, Xue J, Cao Q, Zhang X: **Clinical significance of leukocyte-associated immunoglobulin-like receptor-1 expression in human cervical cancer.** *Exp Ther Med* 2016, **12**(6):3699-3705.
12. Cao Q, Fu A, Yang S, He X, Wang Y, Zhang X, Zhou J, Luan X, Yu W, Xue J: **Leukocyte-associated immunoglobulin-like receptor-1 expressed in epithelial ovarian cancer cells and involved in cell proliferation and invasion.** *Biochem Biophys Res Commun* 2015, **458**(2):399-404.
13. Poggi A, Catellani S, Bruzzone A, Caligaris-Cappio F, Gobbi M, Zocchi MR: **Lack of the leukocyte-associated Ig-like receptor-1 expression in high-risk chronic lymphocytic leukaemia results in the absence of a negative signal regulating kinase activation and cell division.** *Leukemia* 2008, **22**(5):980-988.
14. Singh M, Bhatia P, Shandilya JK, Rawat A, Varma N, Sachdeva MS, Trehan A, Bansal D, Jain R, Totadri S: **Low Expression of Leucocyte Associated Immunoglobulin Like Receptor-1 (LAIR-1/CD305) in a Cohort of Pediatric Acute Lymphoblastic Leukemia Cases.** *Asian Pac J Cancer Prev* 2018, **19**(11):3131-3135.
15. Li W, Wei Z, Liu Y, Li H, Ren R, Tang Y: **Increased 18F-FDG uptake and expression of Glut1 in the EMT transformed breast cancer cells induced by TGF-beta.** *Neoplasma* 2010, **57**(3):234-240.

16. Zhang Y, Ding Y, Huang Y, Zhang C, Jin B, Zhuang R: **Expression of leukocyte-associated immunoglobulin-like receptor-1 (LAIR-1) on osteoclasts and its potential role in rheumatoid arthritis.** *Clinics* 2013, **68**(4):475-481.
17. Meyaard L, Adema GJ, Chang C, Woollatt E, Sutherland GR, Lanier LL, Phillips JH: **LAIR-1, a novel inhibitory receptor expressed on human mononuclear leukocytes.** *Immunity* 1997, **7**(2):283-290.
18. Rygiel TP, Stolte EH, de Ruiter T, van de Weijer ML, Meyaard L: **Tumor-expressed collagens can modulate immune cell function through the inhibitory collagen receptor LAIR-1.** *Molecular immunology* 2011, **49**(1-2):402-406.
19. Yu L, Liu S, Guo W, Zhang C, Zhang B, Yan H, Wu Z: **hTERT promoter activity identifies osteosarcoma cells with increased EMT characteristics.** *Oncol Lett* 2014, **7**(1):239-244.
20. Poudel B, Kim DK, Ki HH, Kwon YB, Lee YM, Kim DK: **Downregulation of ERK signaling impairs U2OS osteosarcoma cell migration in collagen matrix by suppressing MMP9 production.** *Oncol Lett* 2014, **7**(1):215-218.
21. Lei P, Ding D, Xie J, Wang L, Liao Q, Hu Y: **Expression profile of Twist, vascular endothelial growth factor and CD34 in patients with different phases of osteosarcoma.** *Oncol Lett* 2015, **10**(1):417-421.
22. Dong T, Zhang Y, Chen Y, Liu P, An T, Zhang J, Yang H, Zhu W, Yang X: **FOXO1 inhibits the invasion and metastasis of hepatocellular carcinoma by reversing ZEB2-induced epithelial-mesenchymal transition.** *Oncotarget* 2017, **8**(1):1703-1713.
23. Teo Z, Sng MK, Chan JSK, Lim MMK, Li Y, Li L, Phua T, Lee JYH, Tan ZW, Zhu P *et al*: **Elevation of adenylate energy charge by angiopoietin-like 4 enhances epithelial-mesenchymal transition by inducing 14-3-3gamma expression.** *Oncogene* 2017, **36**(46):6408-6419.
24. Nie D, Zheng Q, Liu L, Mao X, Li Z: **Up-regulated of Angiopoietin-Like Protein 4 Predicts Poor Prognosis in Cervical Cancer.** *Journal of Cancer* 2019, **10**(8):1896-1901.
25. Zhang T, Kastrenopoulou A, Larrouture Q, Athanasou NA, Knowles HJ: **Angiopoietin-like 4 promotes osteosarcoma cell proliferation and migration and stimulates osteoclastogenesis.** *BMC cancer* 2018, **18**(1):536.
26. Yang K, Yang Y, Qi C, Ju H: **Effects of porcine STC-1 on cell metabolism and mitochondrial function.** *General and comparative endocrinology* 2019, **286**:113298.
27. Sarapio E, De Souza SK, Model JFA, Trapp M, Da Silva RSM: **Stanniocalcin-1 and -2 effects on glucose and lipid metabolism in white adipose tissue from fed and fasted rats.** *Canadian journal of physiology and pharmacology* 2019, **97**(10):916-923.
28. Schacke M, Kumar J, Colwell N, Hermanson K, Folle GA, Nechaev S, Dhasarathy A, Lafon-Hughes L: **PARP-1/2 Inhibitor Olaparib Prevents or Partially Reverts EMT Induced by TGF-beta in NMuMG Cells.** *International journal of molecular sciences* 2019, **20**(3).
29. Rodriguez MI, Gonzalez-Flores A, Dantzer F, Collard J, de Herreros AG, Oliver FJ: **Poly(ADP-ribose)-dependent regulation of Snail1 protein stability.** *Oncogene* 2011, **30**(42):4365-4372.
30. Masutani M, Fujimori H: **Poly(ADP-ribosyl)ation in carcinogenesis.** *Molecular aspects of medicine* 2013, **34**(6):1202-1216.

31. Shibuya K, Okada M, Suzuki S, Seino M, Seino S, Takeda H, Kitanaka C: **Targeting the facilitative glucose transporter GLUT1 inhibits the self-renewal and tumor-initiating capacity of cancer stem cells.** *Oncotarget* 2015, **6**(2):651-661.
32. Jang M, Kim SS, Lee J: **Cancer cell metabolism: implications for therapeutic targets.** *Experimental & molecular medicine* 2013, **45**:e45.
33. Szablewski L: **Expression of glucose transporters in cancers.** *Biochimica et biophysica acta* 2013, **1835**(2):164-169.

Supplementary File Legend

Supplementary figure 1. Effect of LAIR-1 overexpression on OS cell growth. (A) Western blotting of LAIR-1 expression in hFOB1.19 and OS cell lines. (B) Transfection efficiency at 48 h after overexpressing LAIR-1 (LV-LAIR-1) in HOS cells. Original magnification $\times 200$. (C) *LAIR-1* overexpression efficiency in HOS cells was analyzed by qPCR. *GAPDH* was used as an internal control. ** $P < 0.01$. (D) EdU proliferation assay analysis was performed at 48 h after LV-NC or LV-LAIR-1 lentivirus infection. Untreated HOS cells correspond to the blank group. Cell nuclei were stained with DAPI (blue). Original magnification $\times 200$.

Figures

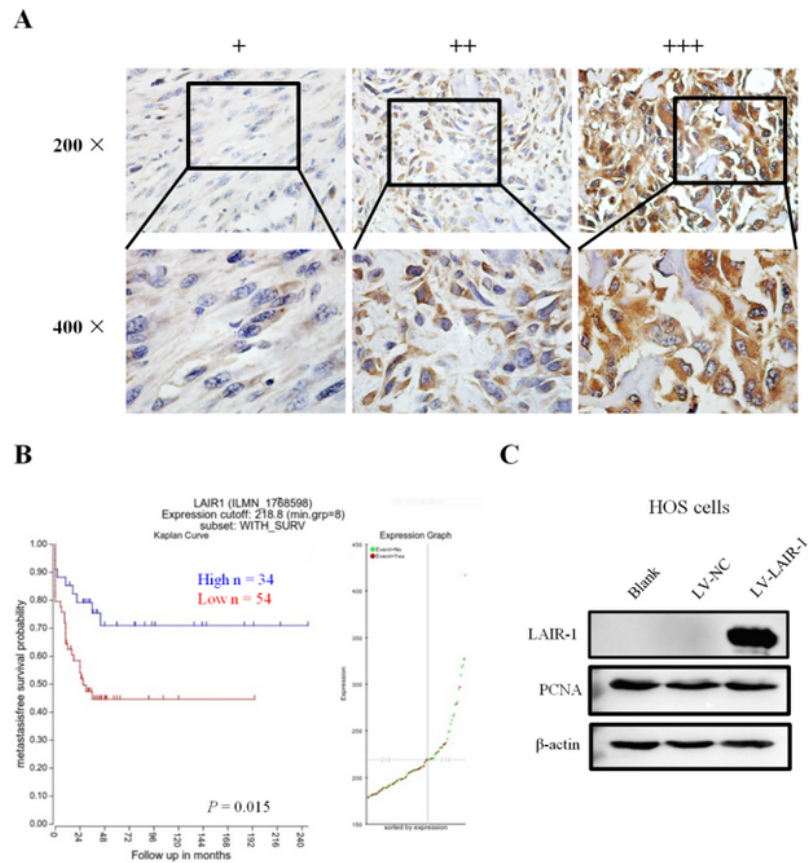


Fig. 1

Figure 1

Representative images of different LAIR-1 immunohistochemistry staining intensities in OS tissues. The percentage of cells staining positive for LAIR-1 was calculated by assessing the entire image. Based on the LAIR-1 staining intensities in OS tumor samples, the staining patterns were categorized as follows: weak (+), moderate (++), and intense (+++). Upper panel, original magnification $\times 200$; lower panel, original magnification $\times 400$. (B) Kaplan-Meier plot of patient survival for tumors with high (blue line) or low (red

line) LAIR-1 expression; data were obtained using the R2 platform. (C) Western blotting of LAIR-1 expression and PCNA proliferation marker in HOS cells following LV-NC or LV-LAIR-1 lentivirus infection or without treatment (blank).

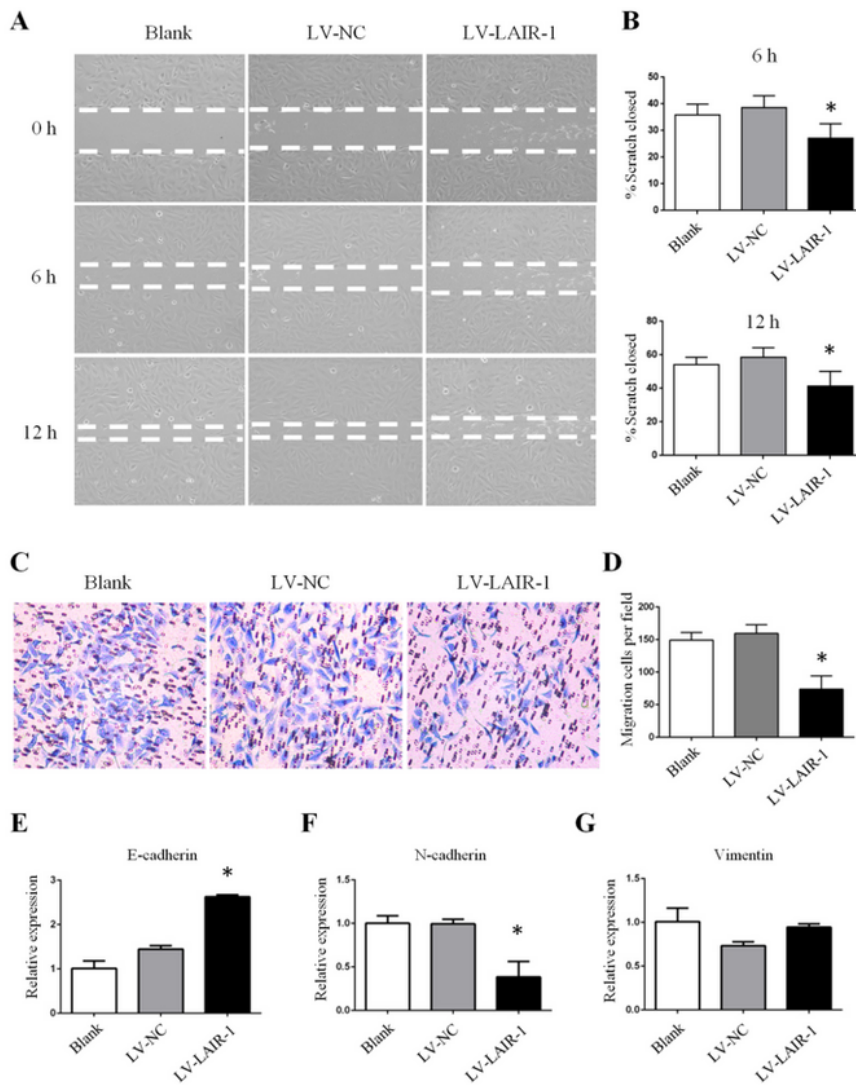


Fig. 2

Figure 2

LAIR-1 overexpression inhibits HOS cell migration. (A) Representative images of cell migration for wound closure. (B) Statistical ratio of wound closure after scratch formation. (C) Representative images of

Transwell membranes stained with crystal violet showing a decreased number of cells after LAIR-1 overexpression. (D) Relative ratio of migratory cells per field. (E-G) LAIR-1 overexpression changes in mRNA expression levels of EMT markers in HOS cells, as determined by qPCR. * P < 0.05.

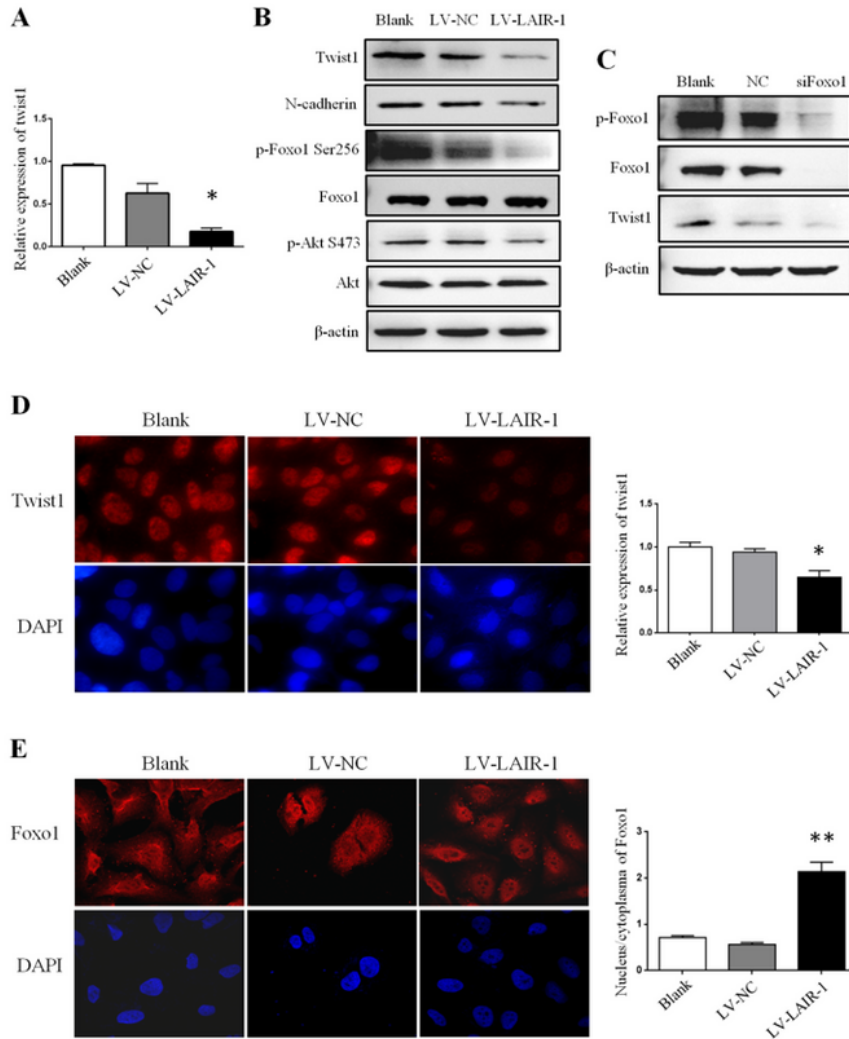


Fig. 3

Figure 3

LAIR-1 overexpression in HOS cells inhibits expression of EMT-associated transcriptional factors by decreasing p-Foxo1 expression. (A) Expression of Twist1 in untreated HOS cells (blank) and

corresponding LV-NC- and LV-LAIR-1-overexpressing transfectants was analyzed by qPCR. (B) Twist1, Slug, p-Foxo1, total Foxo1, p-Akt, and total Akt expression was analyzed by western blotting in blank, LV-NC-overexpressing, and LV-LAIR-1-overexpressing OS cells. (C) Twist1, p-Foxo1, and total Foxo1 expression was analyzed by western blotting in blank, negative control (NC) siRNA, and Foxo1 siRNA (siFoxo1)-transfected OS cells. Representative immunofluorescence staining for Twist1 (D) and Foxo1 (E) in HOS cells (left). Cell nuclei were stained with DAPI (blue). Original magnification $\times 400$. The statistical data for the images are shown in histograms (right). * $P < 0.05$, ** $P < 0.01$. Results represent at least three independent experiments.

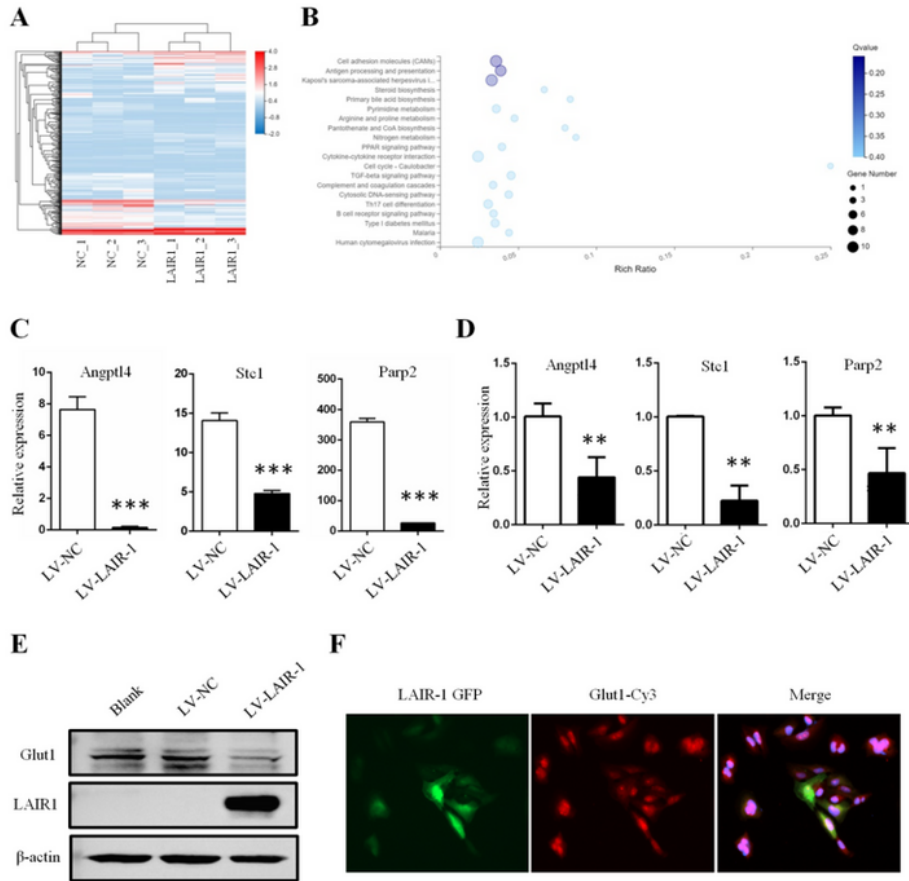


Fig. 4

Figure 4

LAIR-1 inhibits Glut1-related glucose uptake in OS cells. (A) Heatmap showing the levels of differentially expressed mRNAs. (B) Top 20 KEGG pathway annotation categories for target gene functions of predicted mRNAs. (C) Selected significantly differentially expressed mRNA-related to the EMT in RNA-seq data between two groups. *** $P < 0.001$. (D) qPCR validation of differentially expressed EMT-related genes in LV-NC and LV-LAIR-1-overexpressing OS cells, ** $P < 0.01$. (E) Glut1 expression analyzed by

western blotting. (F) Glucose uptake determined by flow cytometric analysis following different treatments. Data were obtained from at least two independent experiments.

Supplementary Files

This is a list of supplementary files associated with this preprint. Click to download.

- [figureS1.docx](#)